13. Influence of engine rotational speed on floor panel vibration

Considering the relation between idle gear rotational speed and engine vibration, which is described in Chapter 11, the investigation on influence of engine rotational speed on floor panel vibration should be conducted. Occupants of the means of transport are exposed on many kinds of vibration determined by different sources and driving conditions. During traffic jam when congestion increases in urban transport all passengers become more often exposed on vibration generated by the idle gear engine. During the drive there are more vibration sources which generate disruptions [43]. The chapter presents results of the research on the influence of engine rotational speed on floor panel vibration as disruptions for the passenger car occupants transferred to the human organism as whole-body vibration via feet.

13.1. Research on vibration propagation paths from engine to car body in locations of penetrate into human body

The scope of research included investigation featuring measurements of vibration acceleration in a three orthogonal directions in locations under the occupant's feet on the floor panel [45]. The vibration signals, being an effect of a force excitation, obtained by working process of engine, were recorded. The vibration in the vehicle structure were excited by engine working on idle gear. It enables to consider only the vibration generated by vehicle mechanism without vibration from road roughness during the drive. The experiment was conducted under laboratory conditions to ensure reproducibility of results.

The research was conducted on the car vehicle which was placed on the special test racks. It allows eliminate the road roughens impact on the suspension and in result to car-body.

13.2. Research results

The established scope of research enables to observe changes of the floor panel vibration for idle gear rotational speed increase. The idle gear rotational speed founded during research were: 750 rpm, 1500 rpm, 2000 rpm and 3000 rpm.

The three orthogonal axes were analyzed separately. The comparison of the acceleration of vibration signals allows determine which directions of the vibration propagation is parent and how the vibration is changing under engine rotational speed increase.

13.2.1. Influence of engine rotational speed on floor panel vibration

The comparison of vibration registered under feet of vehicle occupants for different engine rotational speed are collected in Figs. 13.1-13.12.

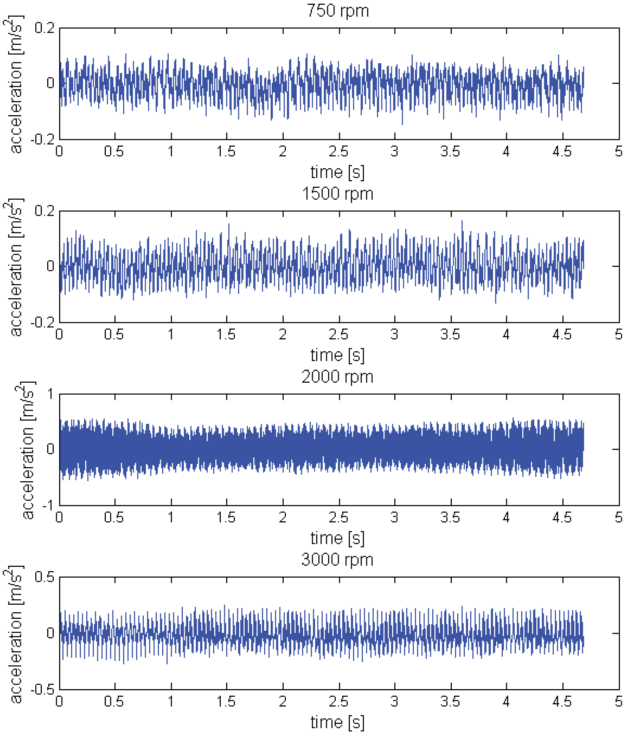

Fig. 13.1. Influence of engine rotational speed on longitudinal vibration of floor panel under driver's feet

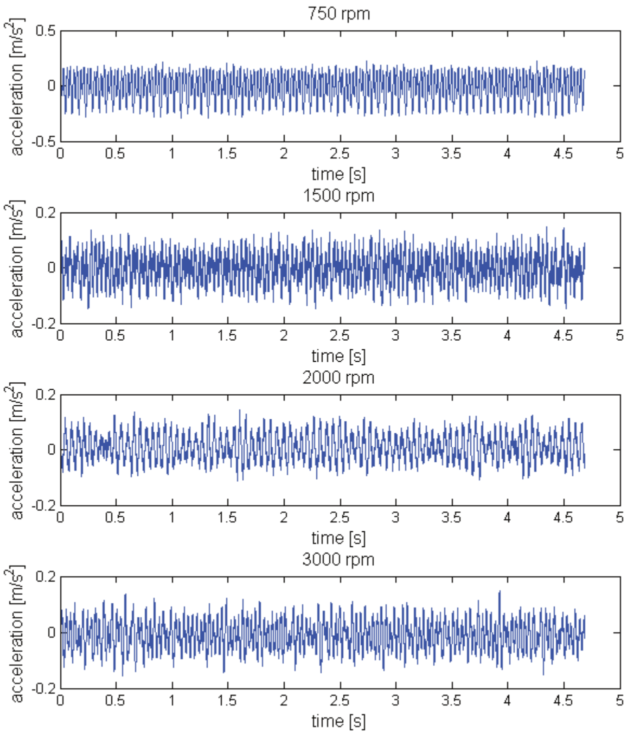

Fig. 13.2. Influence of engine rotational speed on longitudinal vibration of floor panel under front passenger's feet

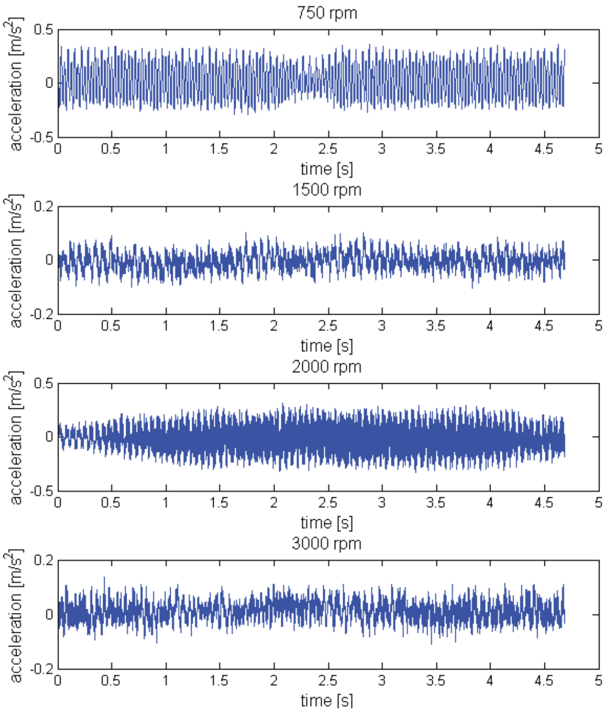

Fig. 13.3. Influence of engine rotational speed on longitudinal vibration of floor panel under rear left passenger's feet

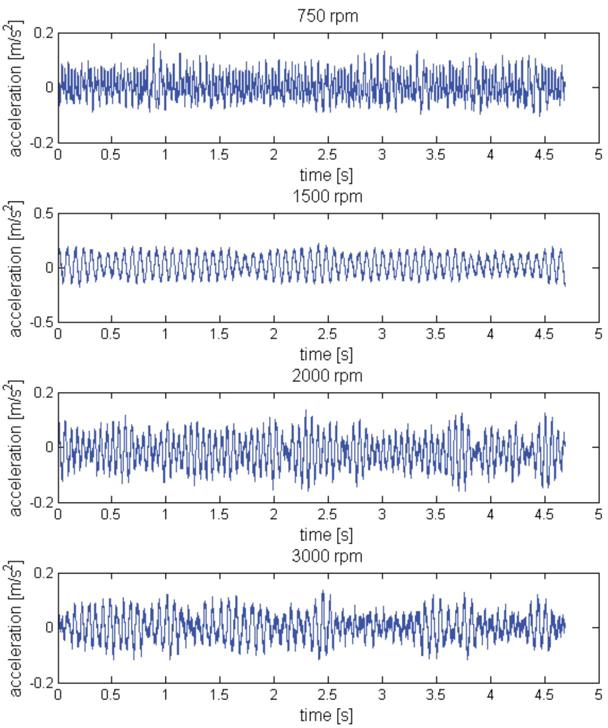

Fig. 13.4. Influence of engine rotational speed on longitudinal vibration of floor panel under rear right passenger's feet

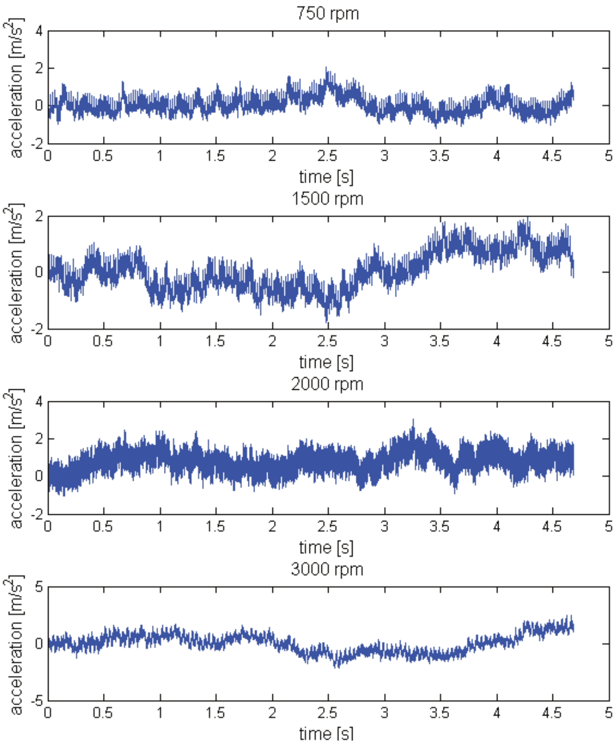

Fig. 13.5. Influence of engine rotational speed on lateral vibration of floor panel under driver's feet

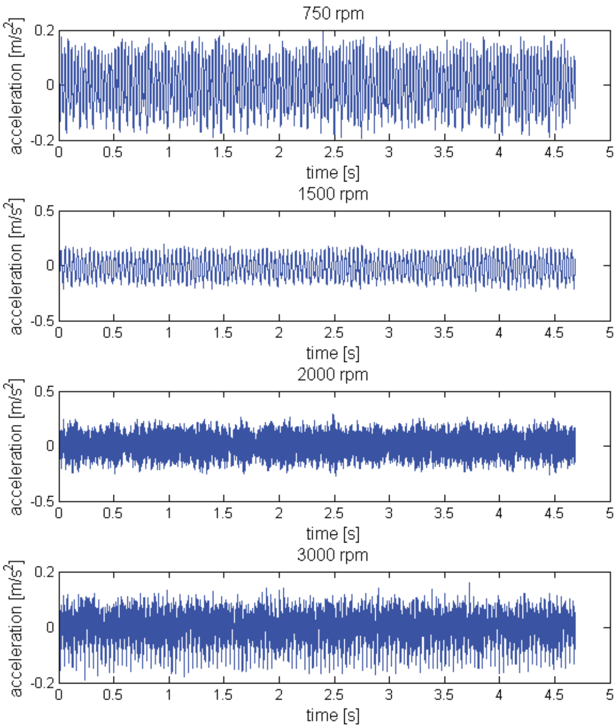

Fig. 13.6. Influence of engine rotational speed on lateral vibration of floor panel under front passenger's feet

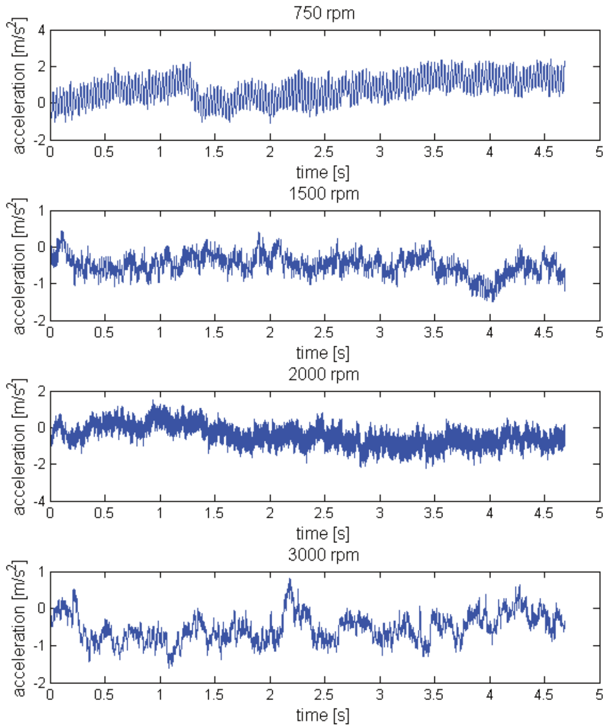

Fig. 13.7. Influence of engine rotational speed on lateral vibration of floor panel under rear left passenger's feet

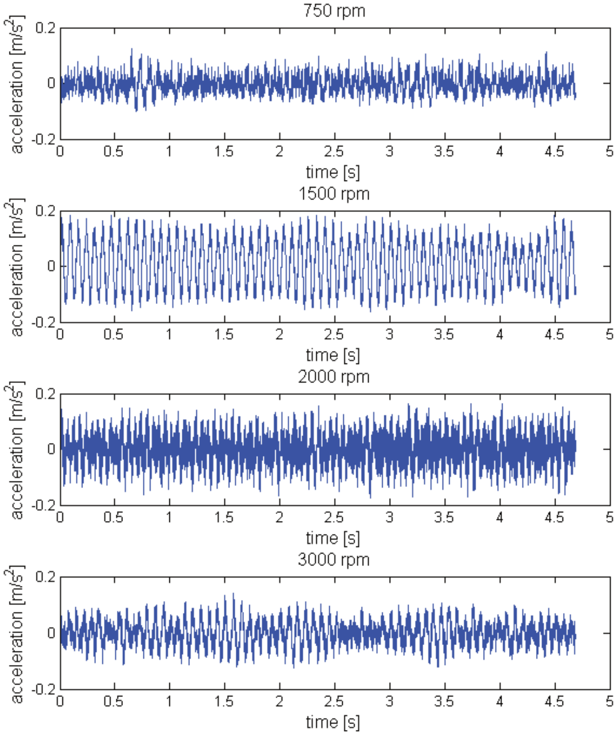

Fig. 13.8. Influence of engine rotational speed on lateral vibration of floor panel under rear right passenger's feet

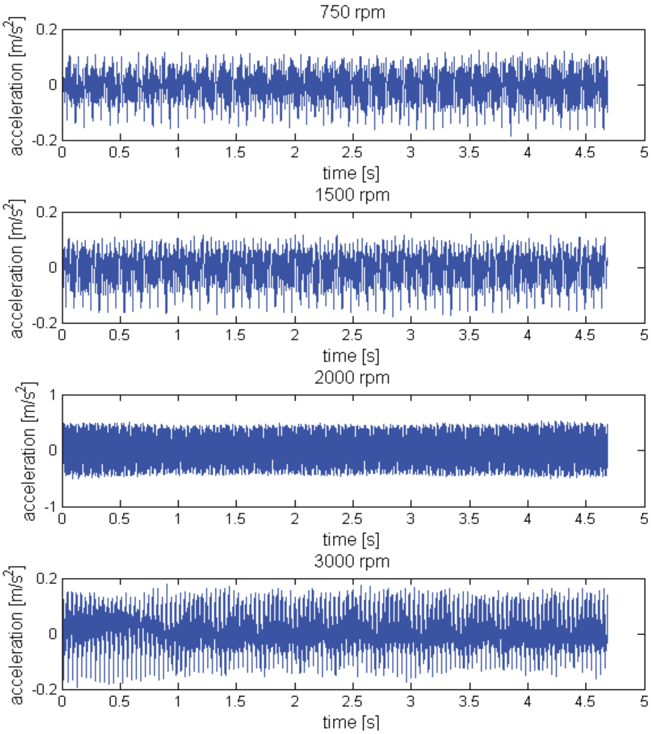

Fig. 13.9. Influence of engine rotational speed on vertical vibration of floor panel under driver's feet

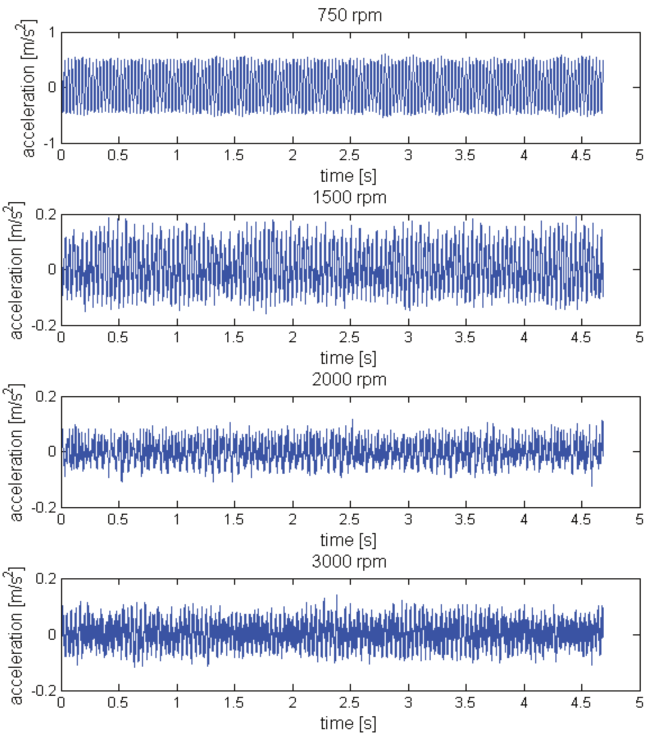

Fig. 13.10. Influence of engine rotational speed on vertical vibration of floor panel under front passenger's feet

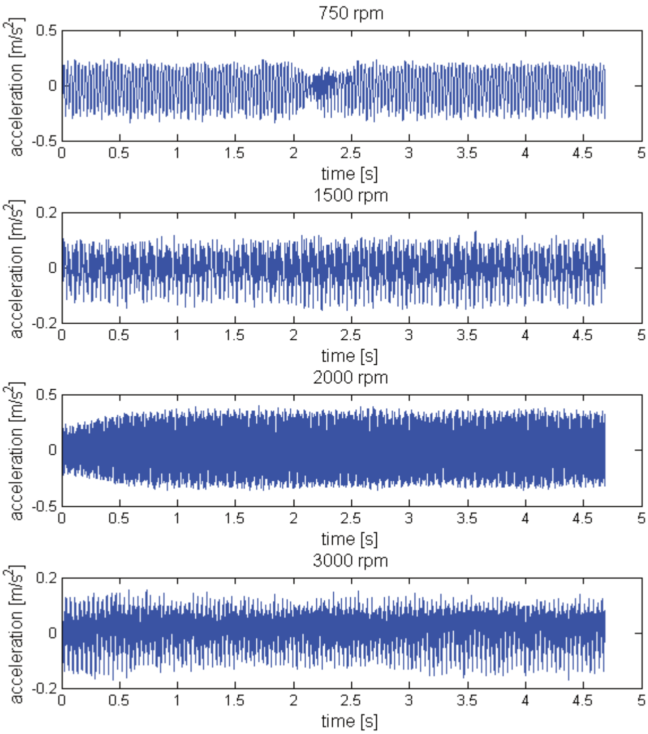

Fig. 13.11. Influence of engine rotational speed on vertical vibration of floor panel under rear left passenger's feet

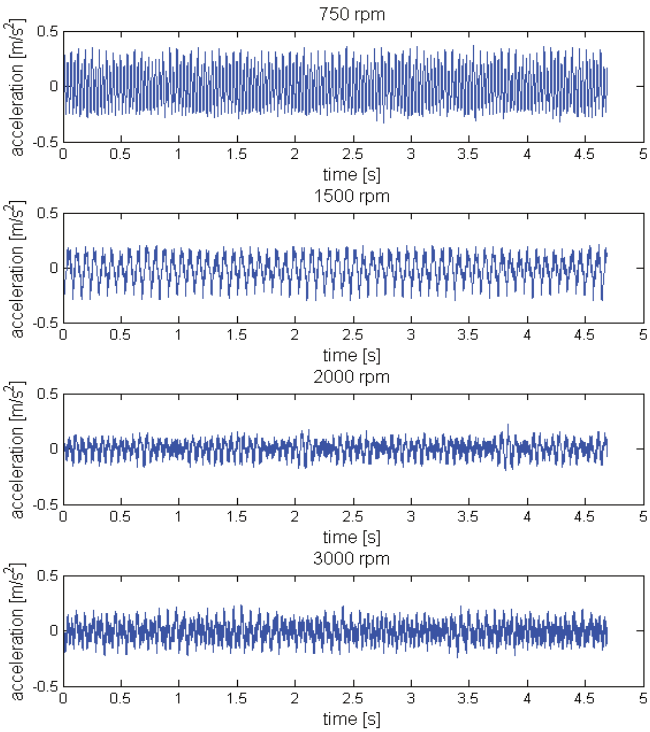

Fig. 13.12. Influence of engine rotational speed on vertical vibration of floor panel under rear right passenger's feet

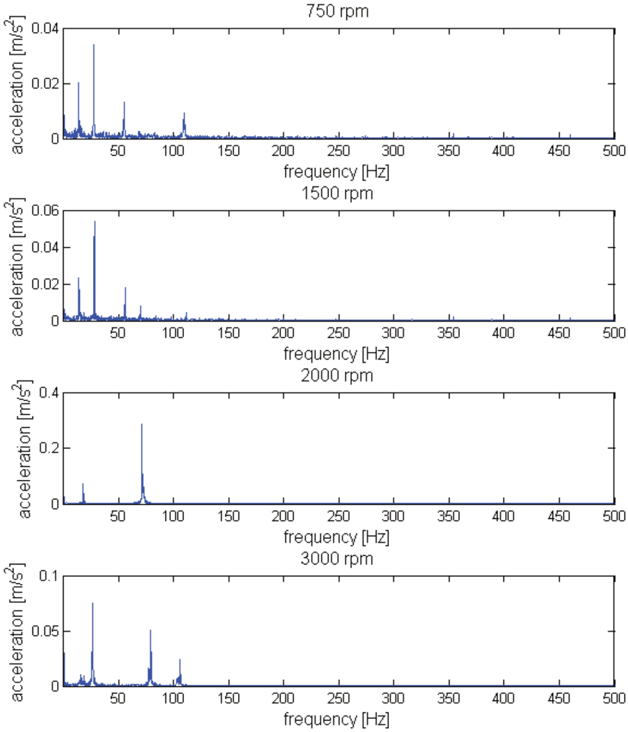

Fig. 13.13. Influence of engine rotational speed on dynamics of longitudinal vibration of floor panel under driver's feet

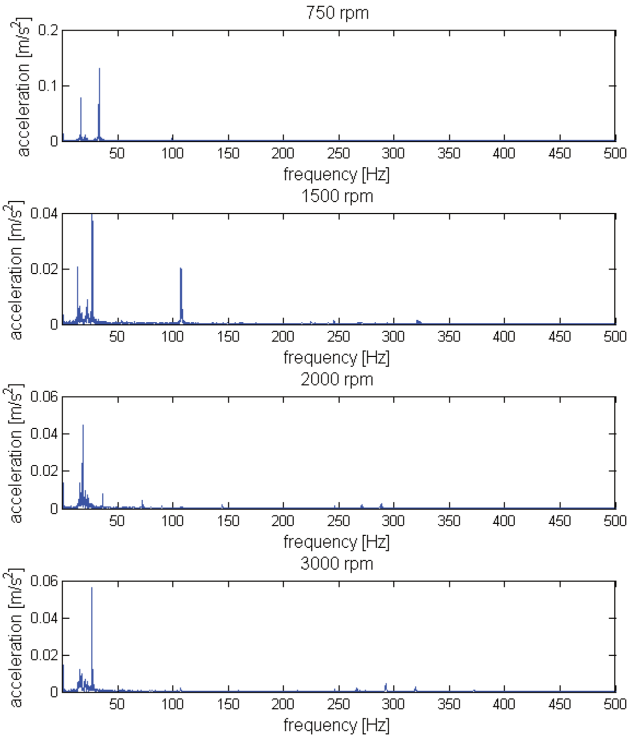

Fig. 13.14. Influence of engine rotational speed on dynamics of longitudinal vibration of floor panel under front passenger's feet

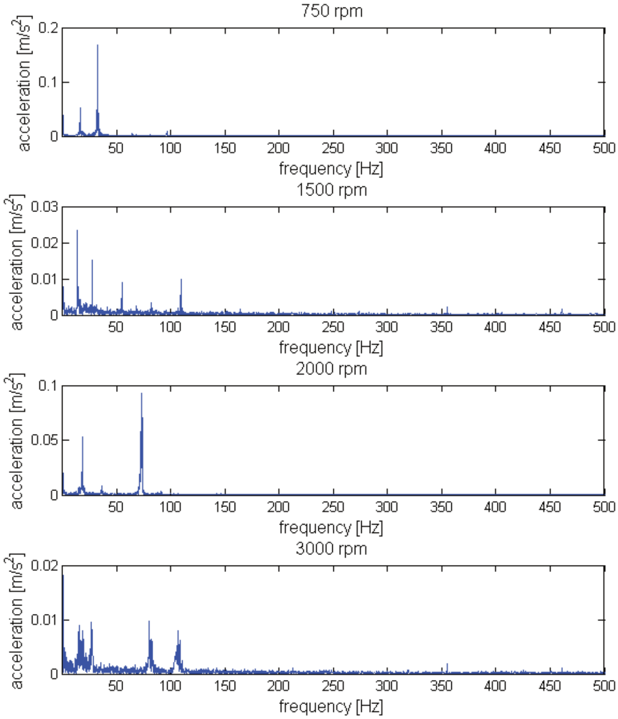

Fig. 13.15. Influence of engine rotational speed on dynamics of longitudinal vibration of floor panel under rear left passenger's feet

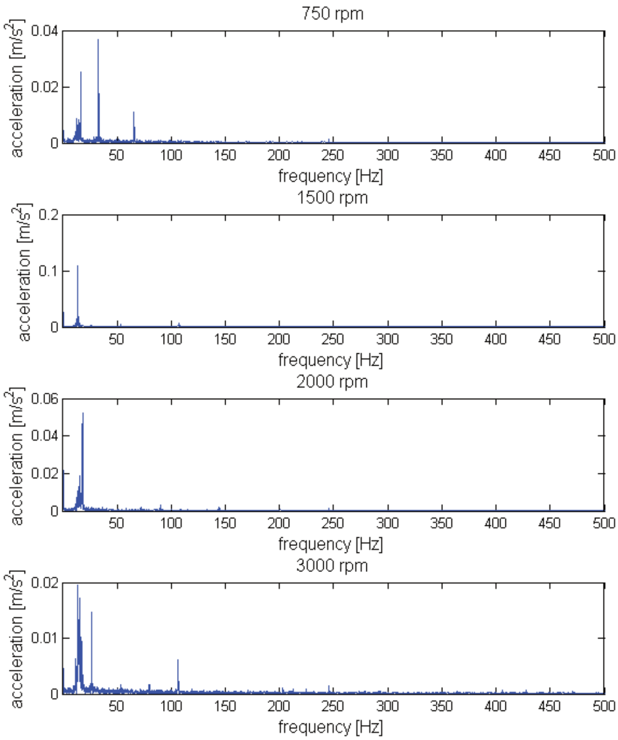

Fig. 13.16. Influence of engine rotational speed on dynamics of longitudinal vibration of floor panel under rear right passenger's feet

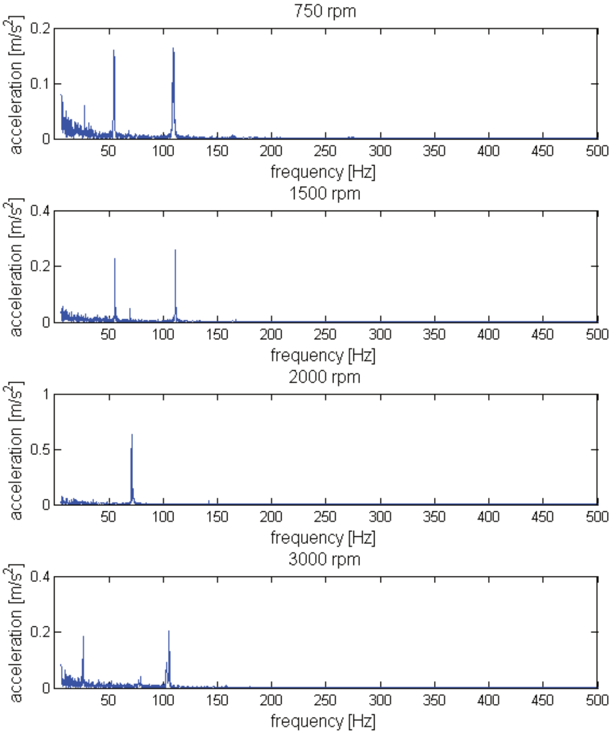

Fig. 13.17. Influence of engine rotational speed on dynamics of lateral vibration of floor panel under driver's feet

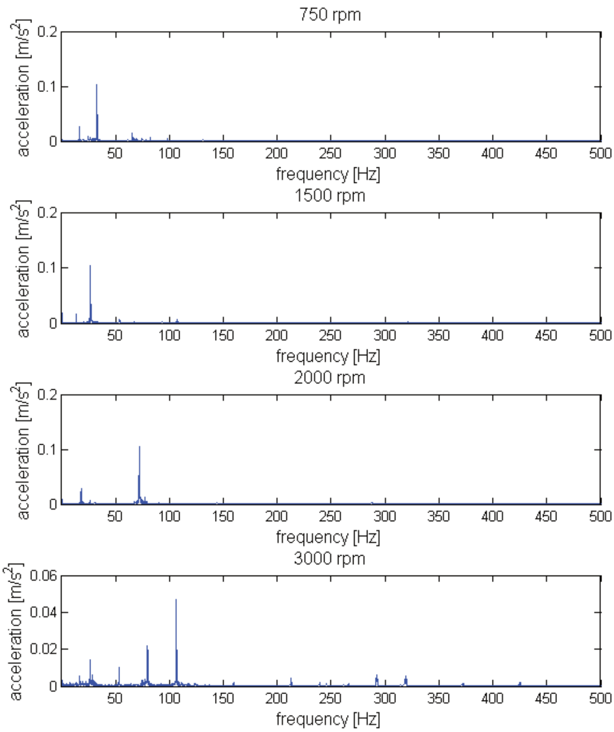

Fig. 13.18. Influence of engine rotational speed on dynamics of lateral vibration of floor panel under front passenger's feet

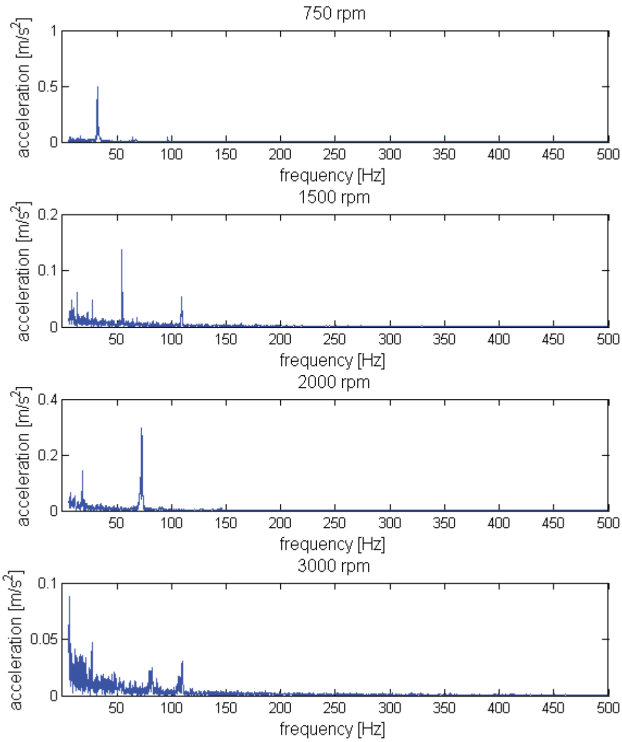

Fig. 13.19. Influence of engine rotational speed on dynamics of lateral vibration of floor panel under rear left passenger's feet

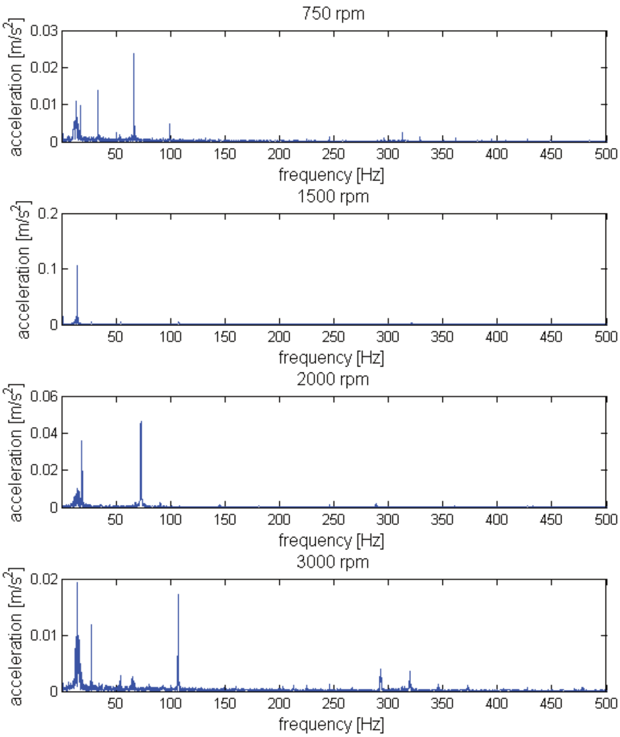

Fig. 13.20. Influence of engine rotational speed on dynamics of lateral vibration of floor panel under rear right passenger's feet

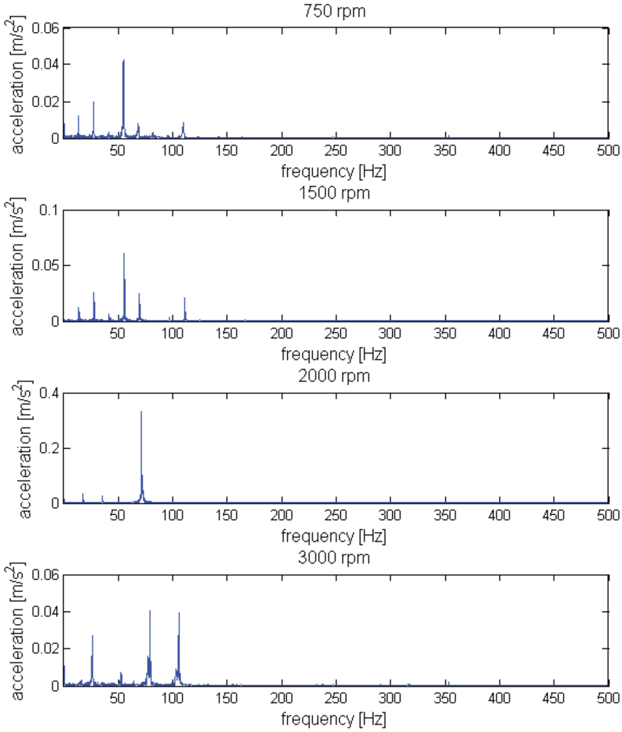

Fig. 13.21. Influence of engine rotational speed on dynamics of vertical vibration of floor panel under driver's feet

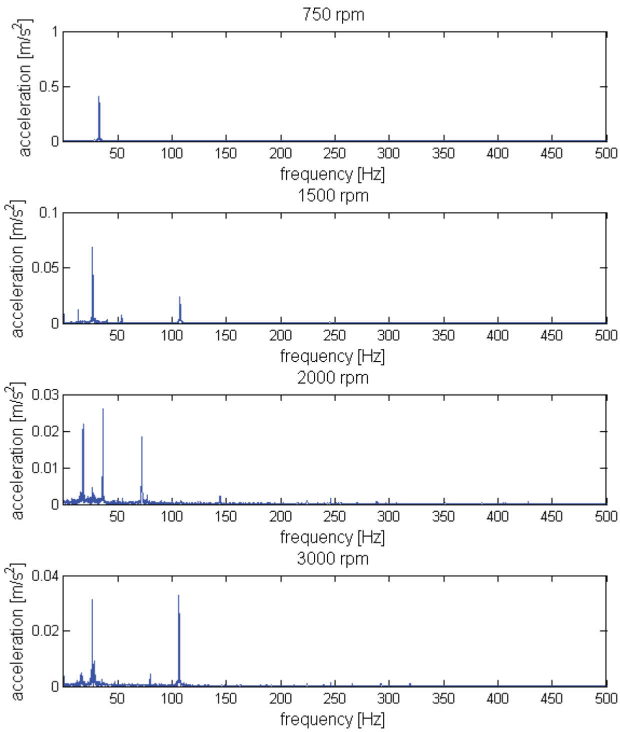

Fig. 13.22. Influence of engine rotational speed on dynamics of vertical vibration of floor panel under front passenger's feet

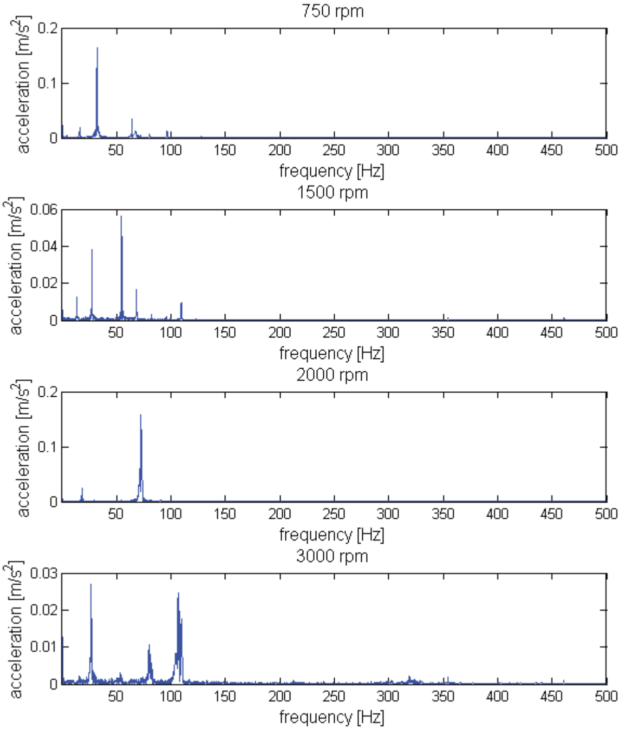

Fig. 13.23. Influence of engine rotational speed on dynamics of vertical vibration of floor panel under rear left passenger's feet

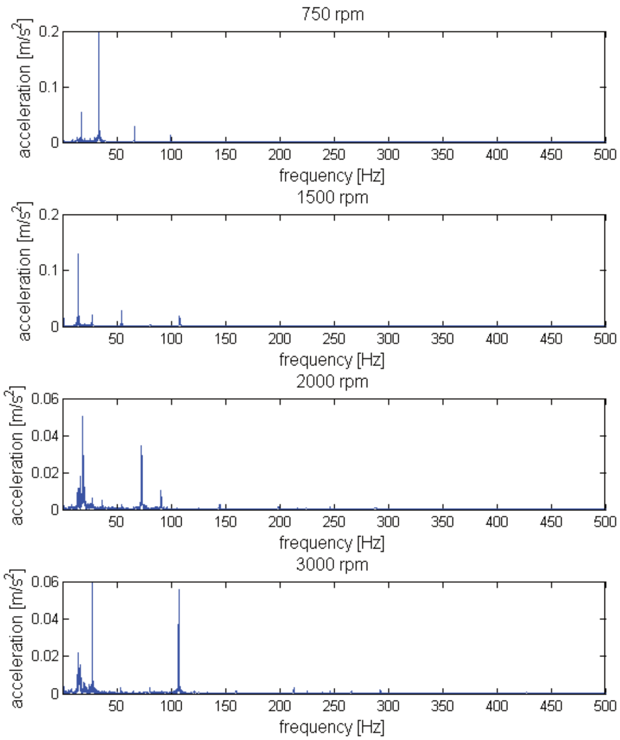

Fig. 13.24. Influence of engine rotational speed on dynamics of vertical vibration of floor panel under rear right passenger's feet

13.2.2. Influence of engine rotational speed on dynamics of floor panel vibration

To investigate this phenomena the spectrum of the recorded signals were determined. It is possible to observe changes of the vibration's dynamics for the different rpm transferred in three orthogonal axes (Figs. 13.13-13.24). The frequency components correlated to rpm were indicated similar to results presented in Fig 11.11. For proper analysis of the vibration amplitude the scale of the *Y* axis have to be taken into consideration.

13.2.3. Influence of engine rotational speed on structure of floor panel vibration

To analyze the influence of engine rotational speed on structure of vibration the time-frequency representation of the signal were determined. For this sake the STFT transformation was calculated. The differences in vibration structure were compared and collected in Figs. 13.25-13.36.

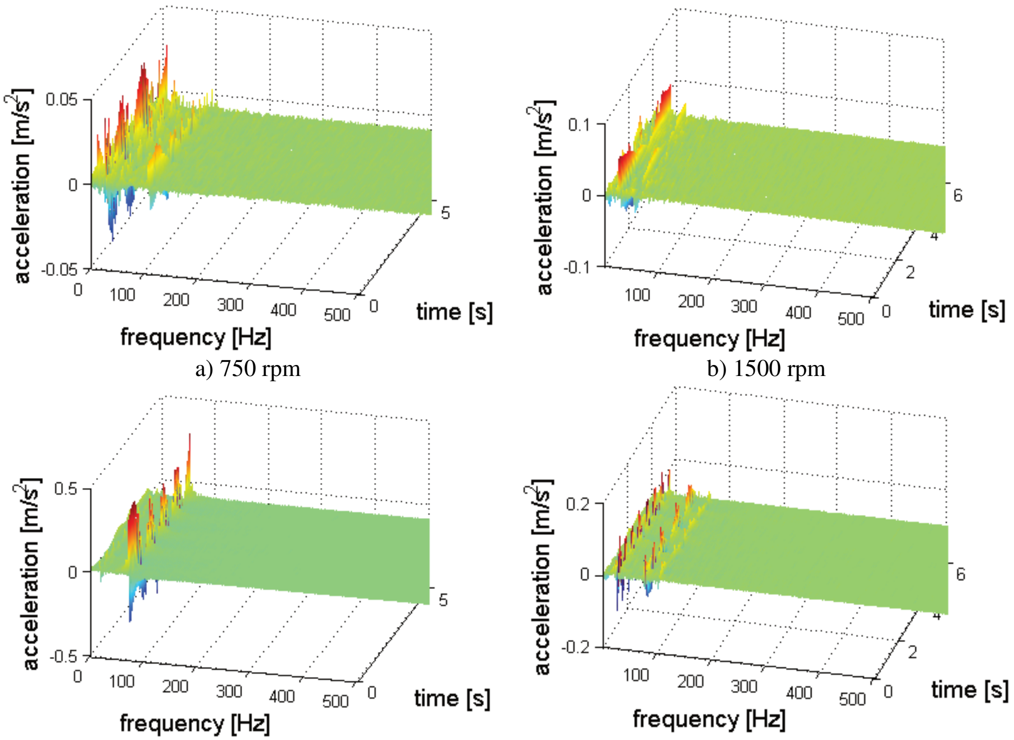

a) 750 rpm b) 1500 rpm

c) 2000 rpm d) 3000 rpm

Fig. 13.25. Changesof structure of longitudinal vibration of floor panel under driver's feet for different engine rotational speed (time window 0.25 s, resoliution 0.4884 Hz)

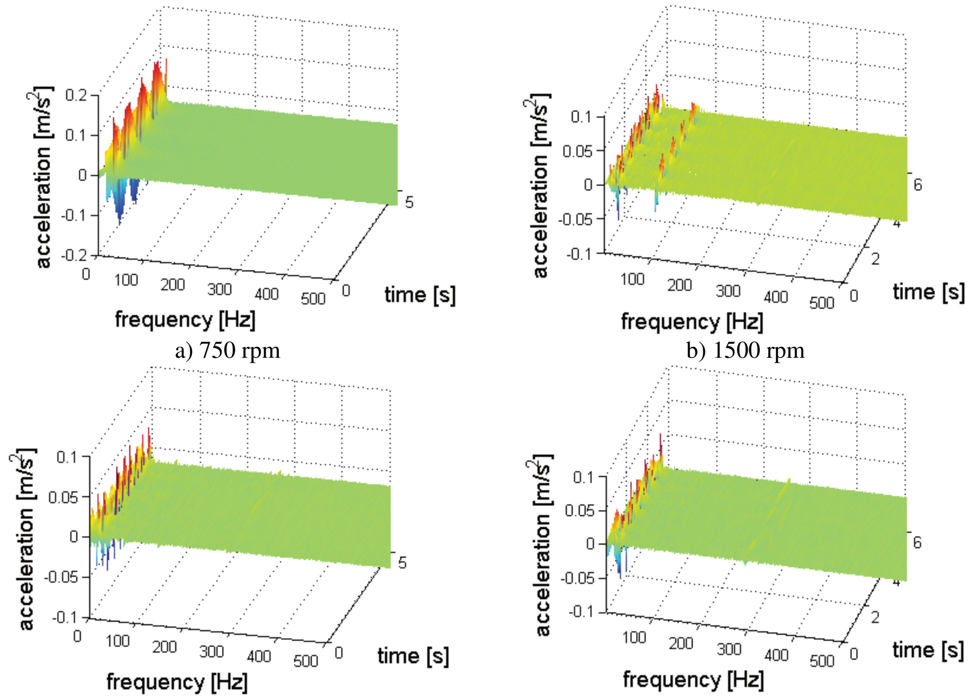

a) 750 rpm b) 1500 rpm

c) 2000 rpm d) 3000 rpm

Fig. 13.26. Changesof structure of longitudinal vibration of floor panel under front passenger's feet for different engine rotational speed (time window 0.25 s, resoliution 0.4884 Hz)

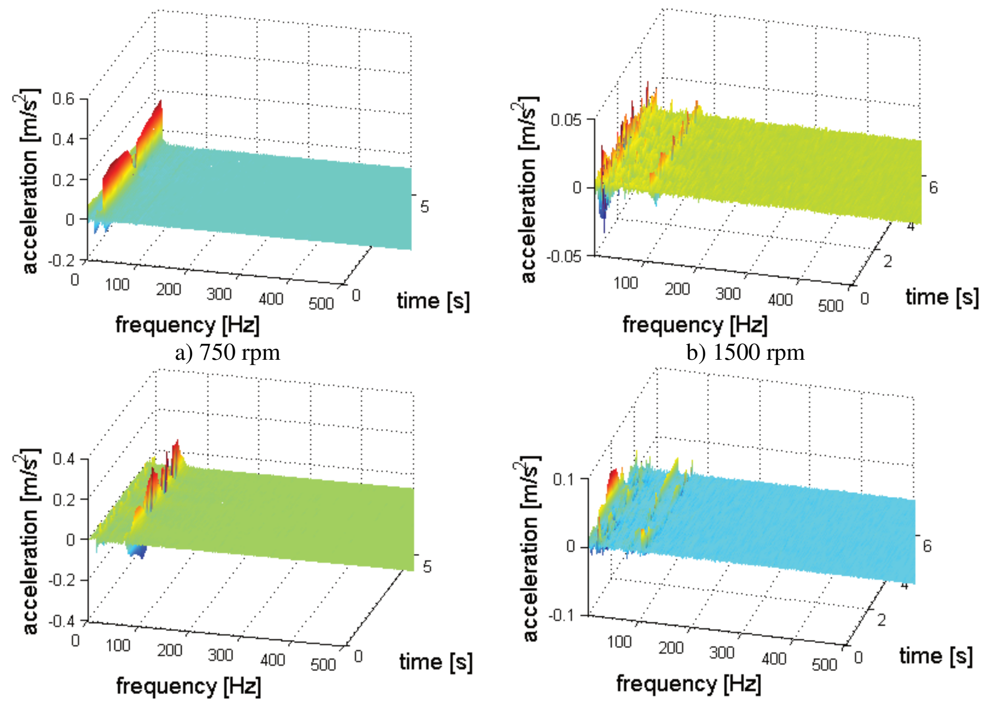

a) 750 rpm b) 1500 rpm

c) 2000 rpm d) 3000 rpm

Fig. 13.27. Changesof structure of longitudinalvibration of floor panel under rear left passenger's feet for different engine rotational speed (time window 0.25 s, resoliution 0.4884 Hz)

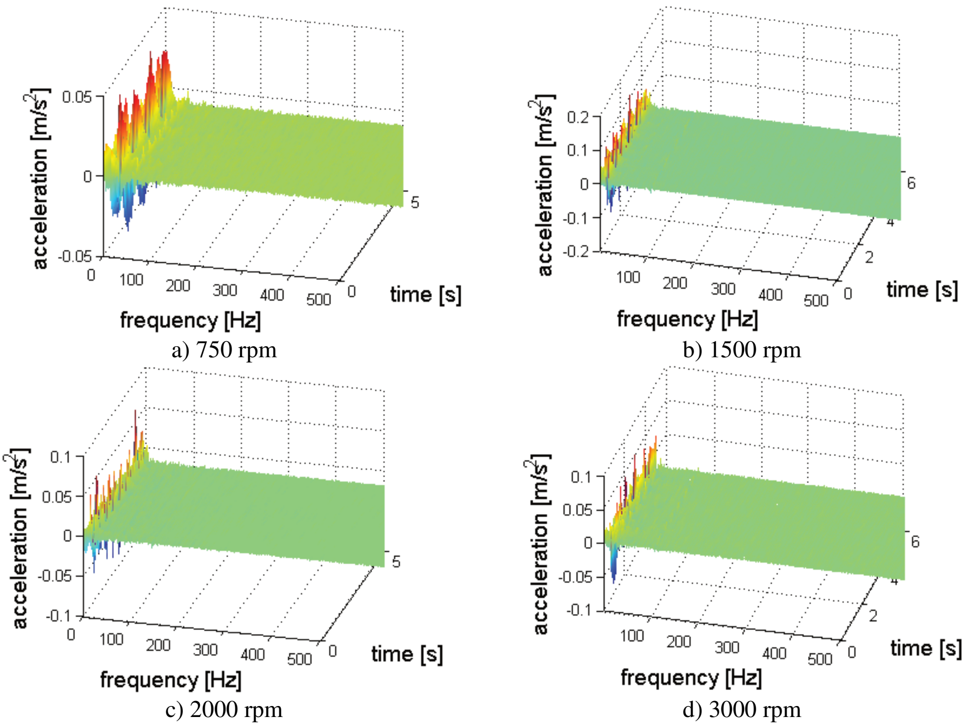

Fig. 13.28. Changesof structure of longitudinalvibration of floor panel under rear right passenger's feet for different engine rotational speed (time window 0.25 s, resoliution 0.4884 Hz)

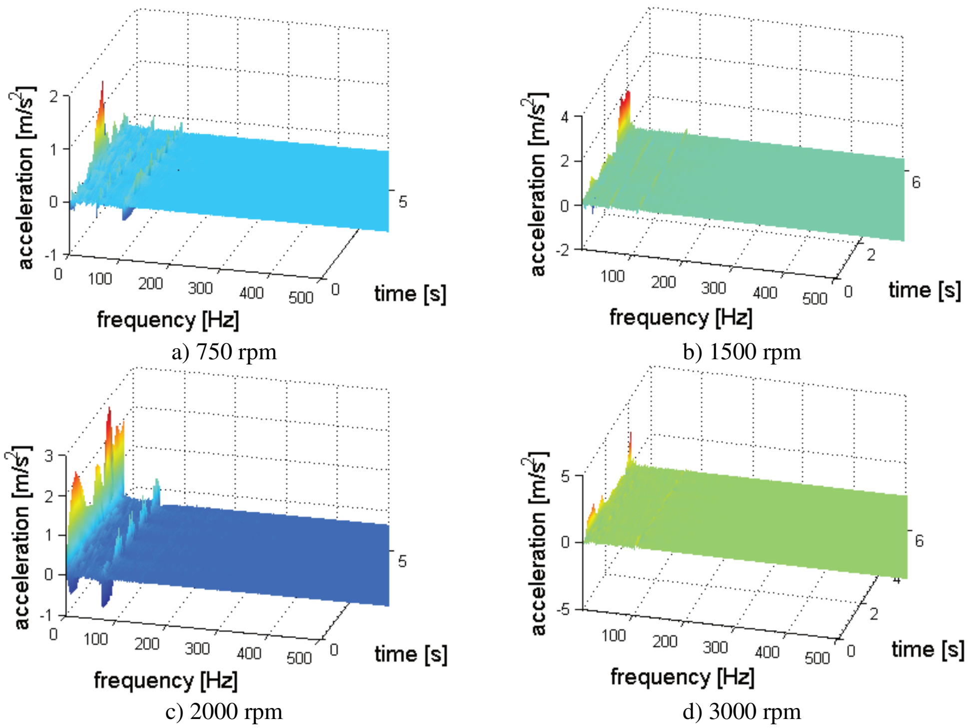

Fig. 13.29. Changesof structure of lateral vibration of floor panel under driver's feet for different engine rotational speed (time window 0.25 s, resoliution 0.4884 Hz)

© JVE INTERNATIONAL LTD. JVE BOOK SERIES ON VIBROENGINEERING. ISSN 2351-5260

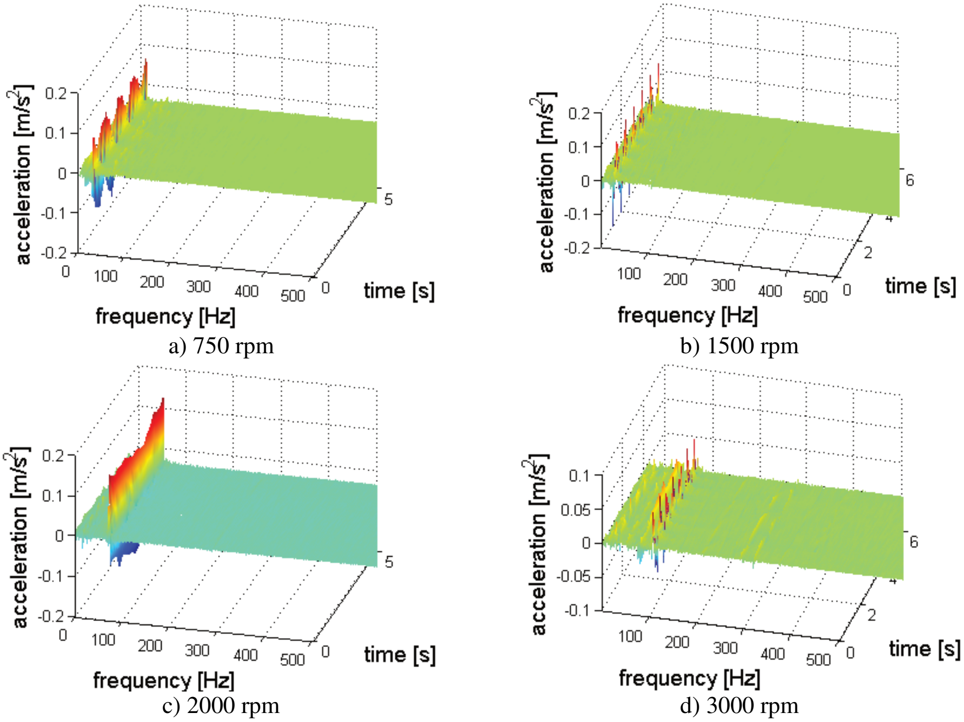

Fig. 13.30. Changesof structure of lateral vibration of floor panel under front passenger's feet for different engine rotational speed (time window 0.25 s, resoliution 0.4884 Hz)

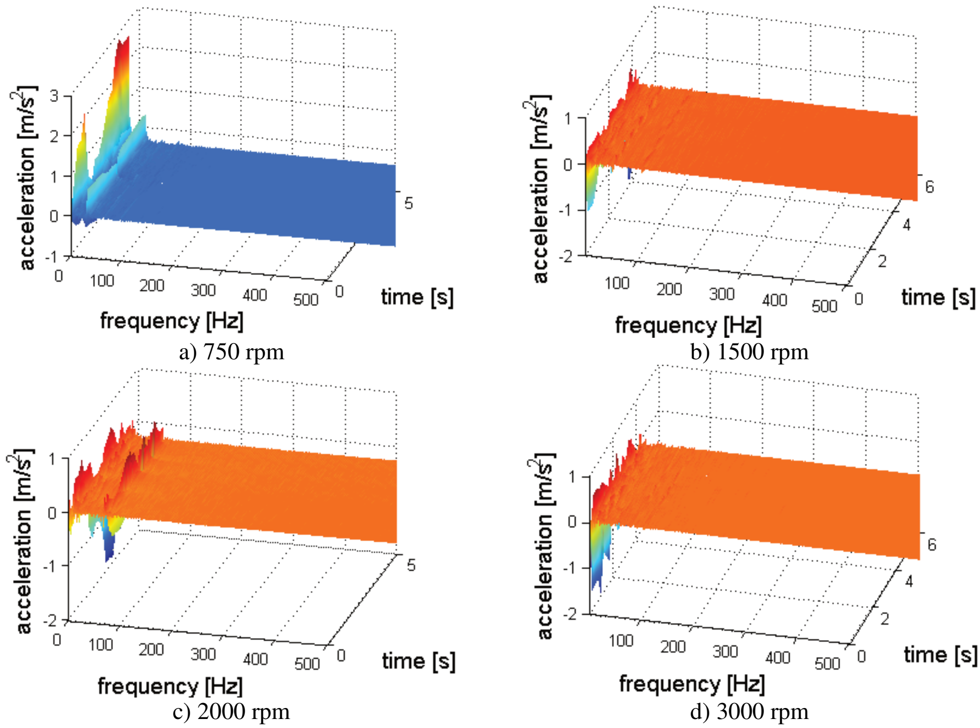

Fig. 13.31. Changesof structure of lateral vibration of floor panel under rear left passenger's feet for different engine rotational speed (time window 0.25 s, resoliution 0.4884 Hz)

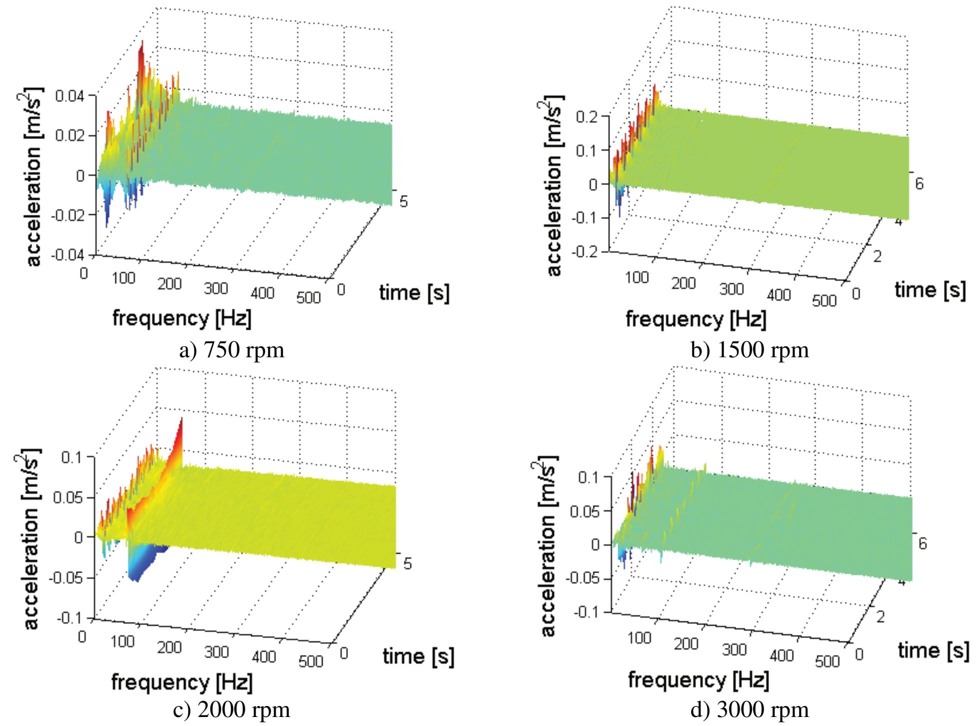

a) 750 rpm b) 1500 rpm

c) 2000 rpm d) 3000 rpm

Fig. 13.32. Changesof structure of lateral vibration of floor panel under rear right passenger's feet for different engine rotational speed (time window 0.25 s, resoliution 0.4884 Hz)

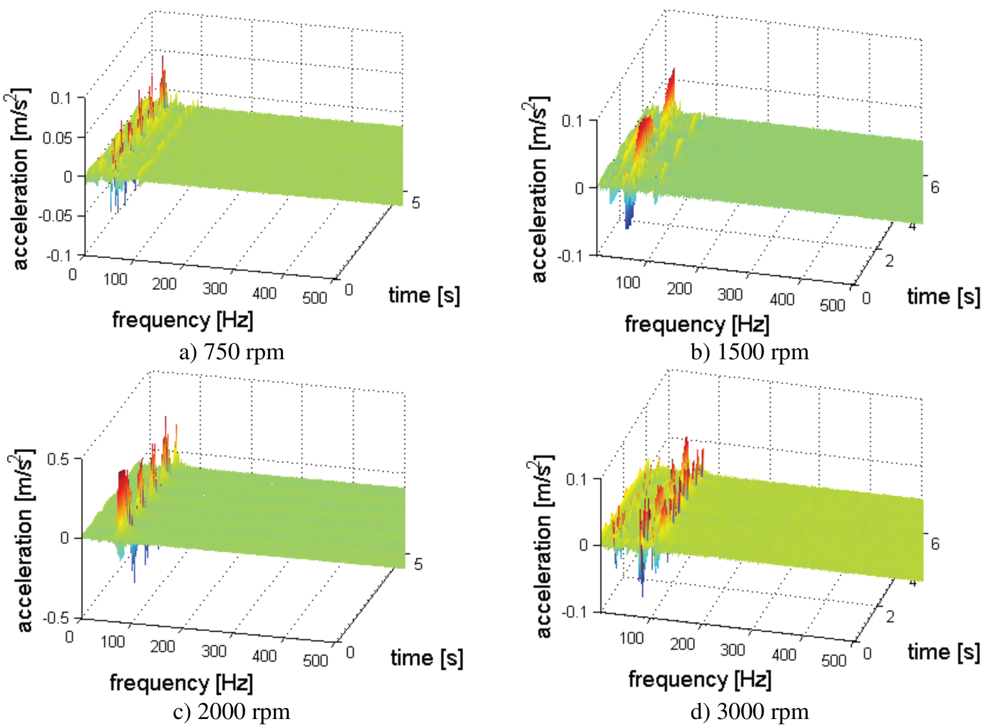

a) 750 rpm b) 1500 rpm

c) 2000 rpm d) 3000 rpm

Fig. 13.33. Changesof structure of vertical vibration of floor panel under driver's feet for different engine rotational speed (time window 0.25 s, resoliution 0.4884 Hz)

© JVE INTERNATIONAL LTD. JVE BOOK SERIES ON VIBROENGINEERING. ISSN 2351-5260

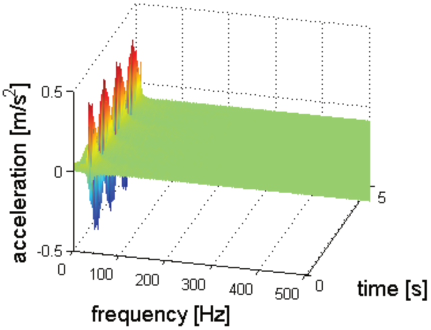

a) 750 rpm

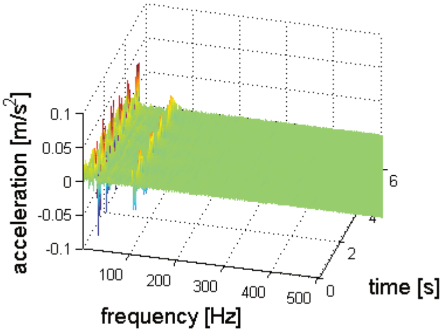

b) 1500 rpm

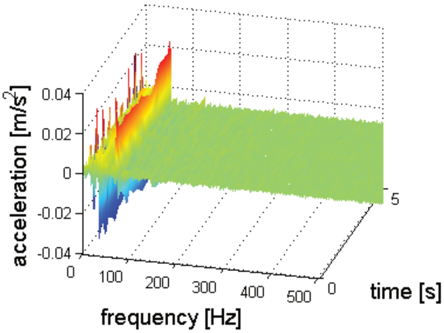

c) 2000 rpm

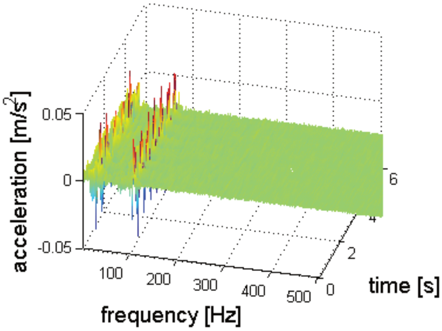

d) 3000 rpm

Fig. 13.34. Changesof structure of vertical vibration of floor panel under front passenger's feet for different engine rotational speed (time window 0.25 s, resoliution 0.4884 Hz)

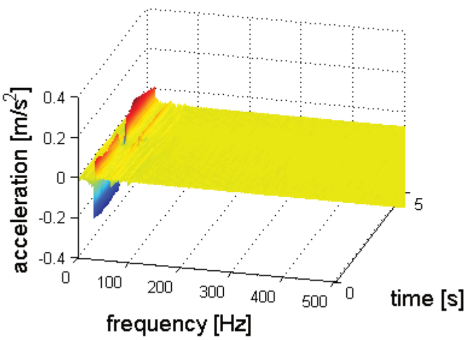

a) 750 rpm

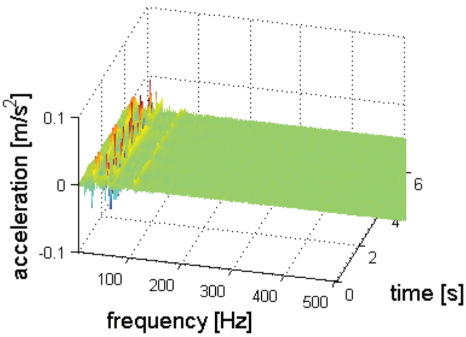

b) 1500 rpm

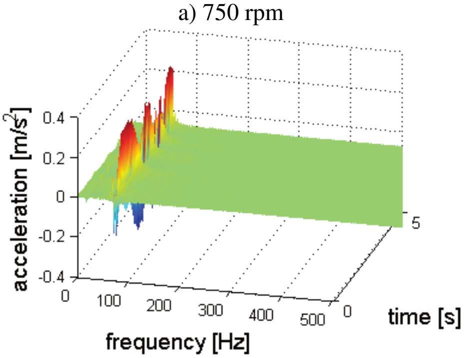

c) 2000 rpm

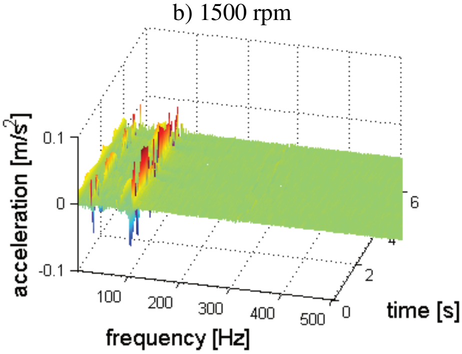

d) 3000 rpm

Fig. 13.35. Changesof structure of vertical vibration of floor panel under rear left passenger's feet for different engine rotational speed (time window 0.25 s, resoliution 0.4884 Hz)

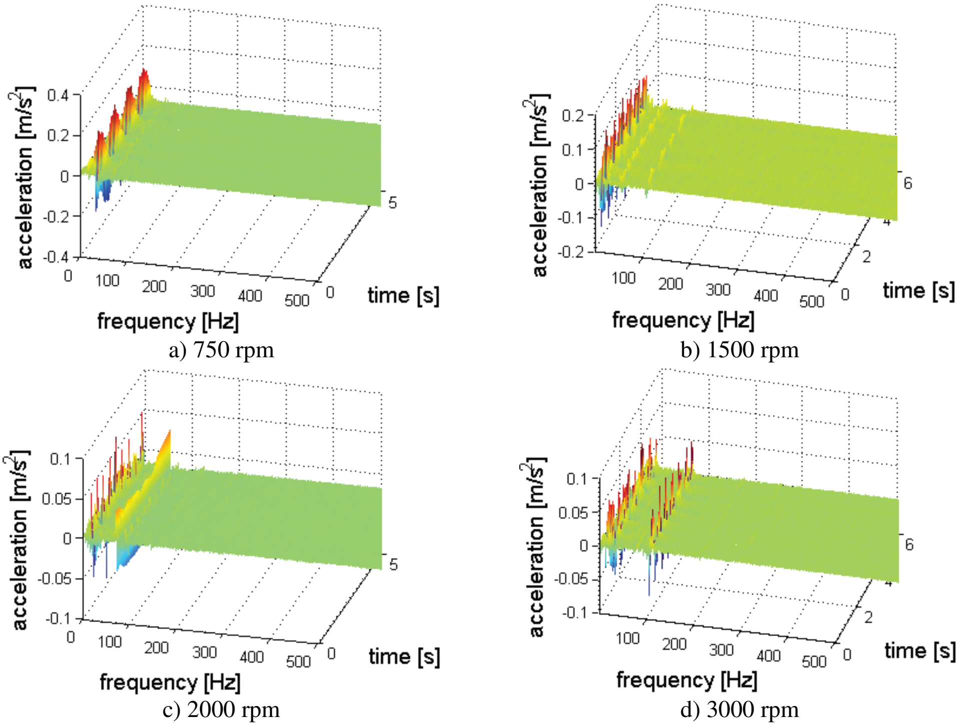

Fig. 13.36. Changesof structure of vertical vibration of floor panel under rear right passenger's feet for different engine rotational speed (time window 0.25 s, resoliution 0.4884 Hz)

13.3. Analysis of engine rotational speed impact on floor panel vibration

To assess exposure to vibrations of the overall impact on the human body by the vibration of the floor panel of the vehicle stopped with working engine the total estimators were calculated. For the analysis of energy of directional distribution of vibrations the RMS values were used. As the energy total estimators it was compared the S_{RMS}, which is expressed as:

$$S_{RMS} = \sum_{i=1}^{n} X_{RMSd_i}, \tag{13.1}$$

where: X_{RMS} – root mean square of vibration signal, i – number of different exposure type, d – direction (x – longitudinal, y – lateral, z – vertical), n – total number of exposure type.

The distribution of these estimators are shown in Fig. 13.37.

What's most interesting in analysis results is that the energy estimators have larger values for the smallest idle gear rotational speed. The analysis of vibration signal energy value correlated to frequency distribution based on defined estimator can be more sensitive to exposure and perception on human vibration. Thus the estimator of energy of vibration spectrum for separate direction was proposed and determined by equation:

$$T_{abs(FFT)} = \frac{1}{D} \sum_{i}^{NFFT/2} |FFT(i)|, \tag{13.2}$$

where: $NFFT$ – number of Fast Fourier Transform samples, D – standardizing parameter (i.e. $D = 100$), $FFT(i)$ – ith component of Fast Fourier Transform, i – next sample of FFT.

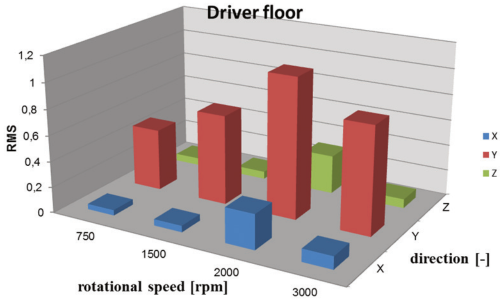

a) Driver floor RMS

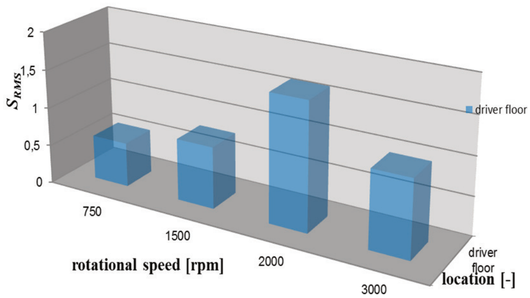

b) Driver floor S_{RMS}

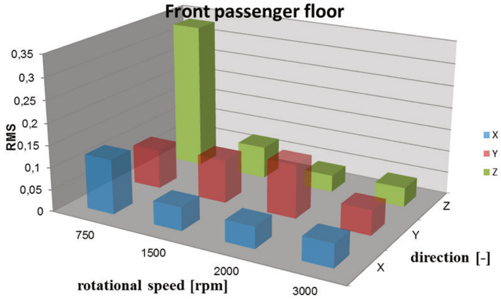

c) Front passenger floor RMS

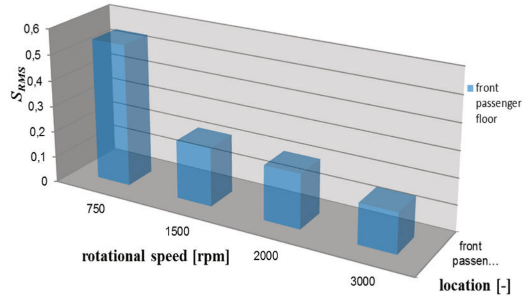

d) Front passenger floor S_{RMS}

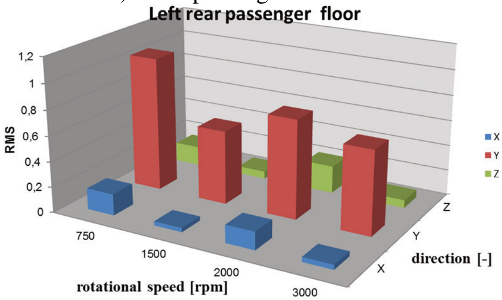

e) Left rear passenger floor RMS

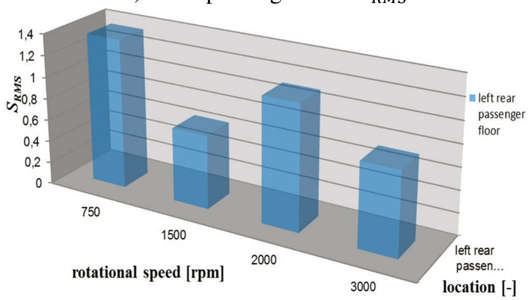

f) Left rear passenger floor S_{RMS}

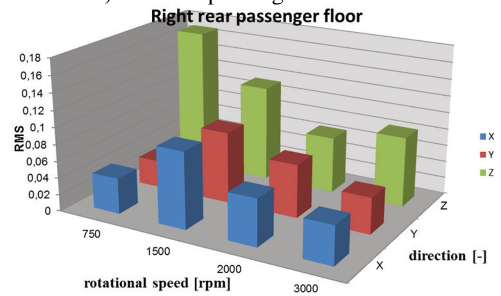

g) Right rear passenger floor RMS

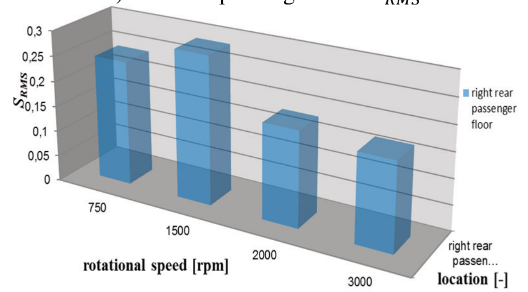

h) Right rear passenger floor S_{RMS}

Fig. 13.37. Distribution of time energy floor panel vibration estimators RMS and S_{RMS} for different engine rotational speed

As the total energy of vibration spectrum the S_{Tabs} estimator was proposed and expressed as:

$$S_{Tabs} = \sum_{i=1}^{n} T_{abs(FFT)_{d_i}}. \tag{13.3}$$

Figs. 13.38-13.39 present the distribution of these frequency estimators.

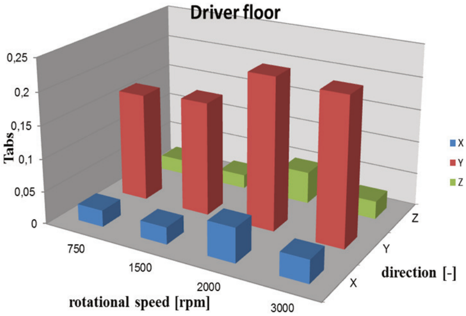

a) Driver floor $T_{abs(FFT)}$

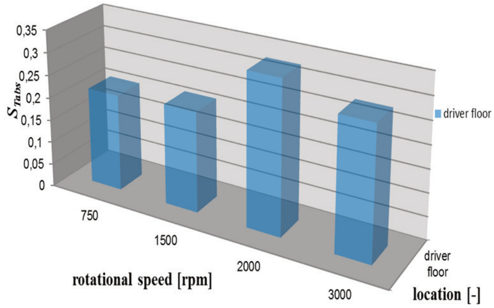

b) Driver floor S_{Tabs}

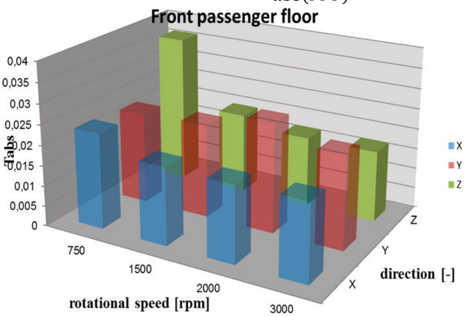

c) Front passenger floor $T_{abs(FFT)}$

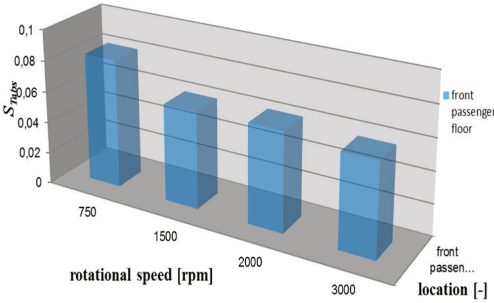

d) Front passenger floor S_{Tabs}

Fig. 13.38. Distribution of frequency energy front floor panel vibration estimators $T_{abs(FFT)}$ and S_{Tabs} for different engine rotational speed

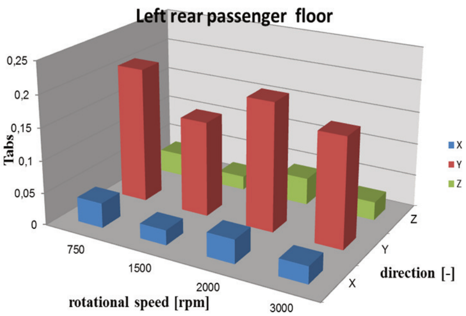

e) Left rear passenger floor RMS

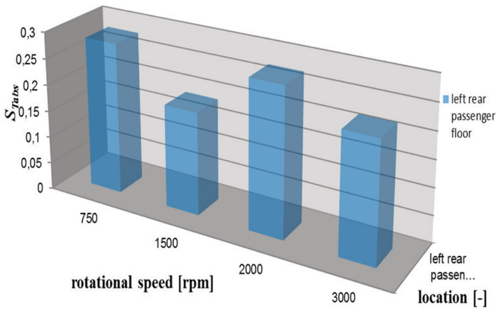

f) Left rear passenger floor S_{RMS}

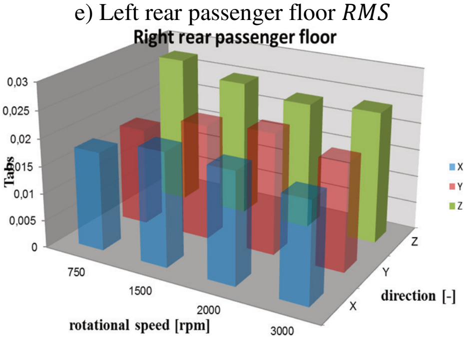

g) Right rear passenger floor RMS

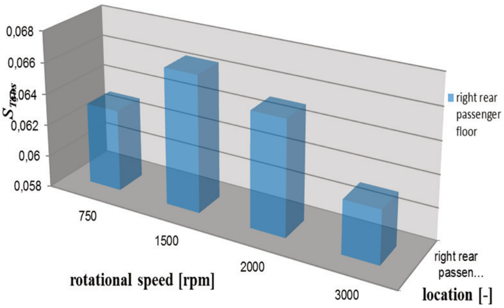

h) Right rear passenger floor S_{RMS}

Fig. 13.39. Distribution of frequency energy rearfloor panel vibration estimators $T_{abs(FFT)}$ and S_{Tabs} for different engine rotational speed

Analysing of engine rotational speed influence on structure of vibration presented as TFR the method of TFR energy estimator were developed. This method enables determining the energy of

TFR of vibration estimator expressed as:

$$T_{absTFR} = \frac{1}{D} \sum_{i}^{NFFT/2} |FFT(X_{RMS}(TFR(i,t))|, \tag{13.4}$$

where: $X_{RMS}(TFR(i,t))$ – root mean square of time distribution of ith frequency component of TFR, t – next sample of time (correlated with time window of TFR method).

The developed method is illustrated in Fig. 13.40. From TFR of the vibration signal next time distributions of the frequency component of the TFR are determined and the RMS of these distributions are calculated. As the result the frequency distribution of RMS of time components of TFR are obtained (Fig. 13.41). Thus the estimator of energy of vibration RMS spectrum can be determined.

As the total energy of TFR of vibration the $S_{TabsTFR}$ estimator is proposed and can be expressed as:

$$S_{TabsTFR} = \sum_{i=1}^{n} T_{absTFR\,d_i}. \tag{13.5}$$

Fig. 13.42 present the distribution of these TFR estimators.

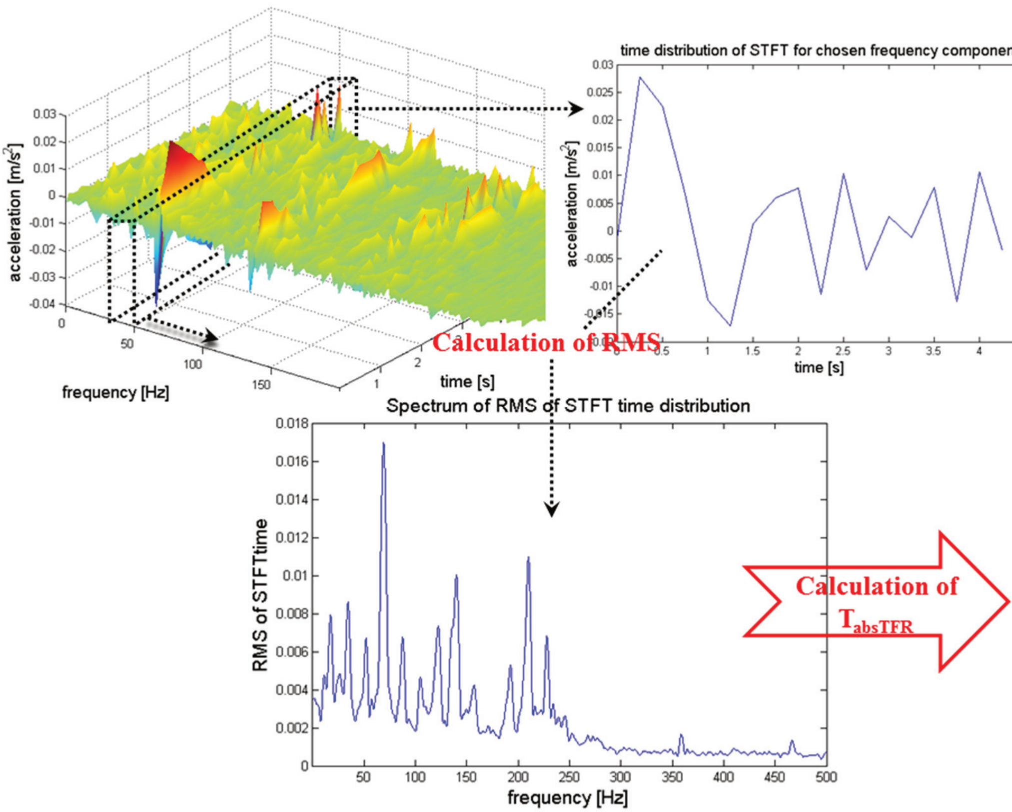

Fig. 13.40. Illustration of the method for the estimation of energy of TFR of vibration (T_{absTFR}) determination

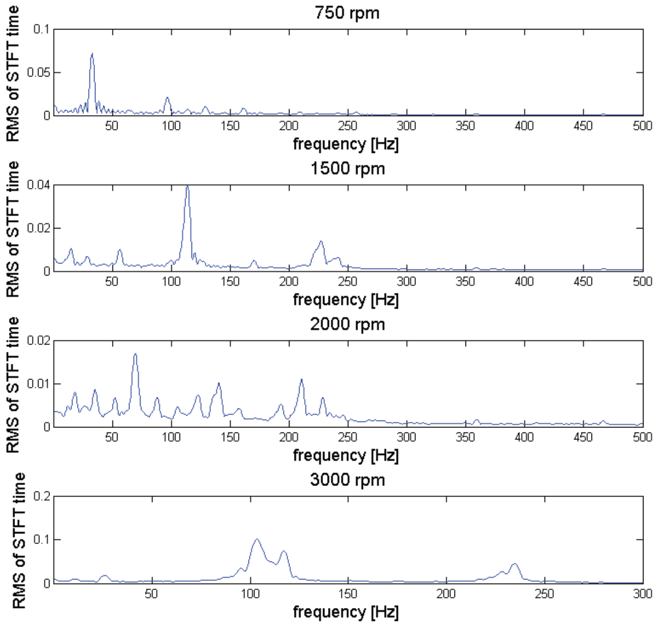

Fig. 13.41. Example of frequency distribution of RMS of time components of TFR of vibration on the floor panel under the driver's feet

13.4. Result and functions analysis

Results obtained show that increase of the engine rotational speed is not directly proportional to generated floor panel vibration. The analysis of the signal's spectrums allows to clearly identify the frequency components correlated to engine rotational speed.

In conclusion of results analysis some interesting observations were obtained. The vibration penetration into the driver via feet registered on the floor panel have unstable dynamic structure. Based on the spectrums analysis it can be observed that due to the increase of rotational speed the floor panel vibration have more frequency components. For the spectrum of the idle gear vibration the energy is focused around one major frequency component.

The TFR of vibration occurring due to increase of engine rotational speed shown some interesting phenomena in vibration structure. The time distribution for main frequency component become more inconstant for occurring and shifting in the time when main frequency vibration are lower to the other frequency components.

For the purpose of assessing exposure to vibrations of the overall impact on the human body by the vibration of the floor panel of the standing vehicle with working engine the total estimators were proposed and compared. Distribution of time energy floor panel vibration estimators RMS and S_{RMS} for different engine rotational speed shows that the energy estimators can have larger values for the smallest idle gear rotational speed. It is correlated to the feeling of vibration discomfort in the traffic jam, when engine is working on idle gear. To consider the influence on the dynamic of the vibration due to increase of the dynamic of the source the frequency estimators $T_{abs(FFT)}$ and S_{Tabs} were developed. The directional distribution of $T_{abs(FFT)}$ is different than RMS but the S_{Tabs} distribution is much more similar to the S_{RMS}. Some differences in sensitivity on engine rotational speed of those estimators can be observed. The most complex analysis of influence of engine rotational speed on floor panel vibration can be conducted basing on TFR of the signals. Thus the method of TFR energy estimator was developed. It allows to calculate the estimator depends on time and frequency distribution of the vibration. Thus the estimator of energy of vibration RMS spectrum can be determined as $T_{abs(FFT)}$ for directional propagation and $S_{TabsTFR}$ for total vibration energy.

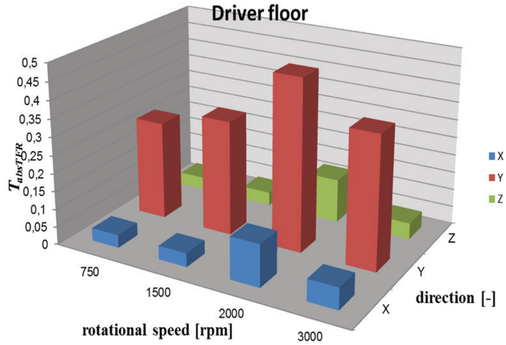

a) Driver floor T_{absTFR}

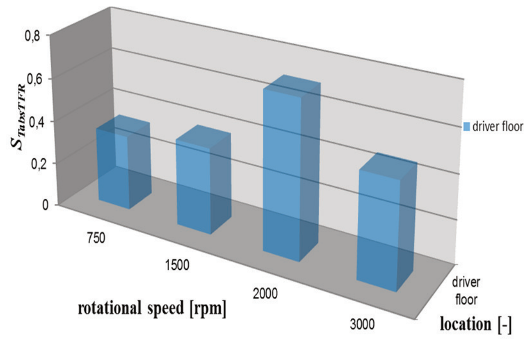

b) Driver floor $S_{TabsTFR}$

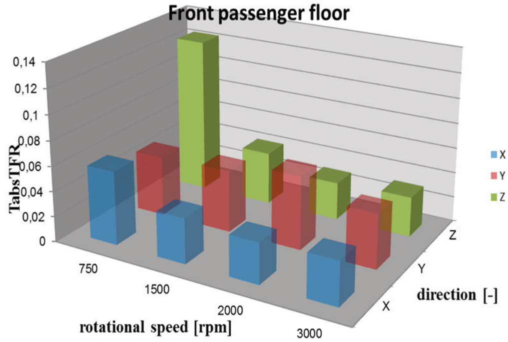

c) Front passenger floor T_{absTFR}

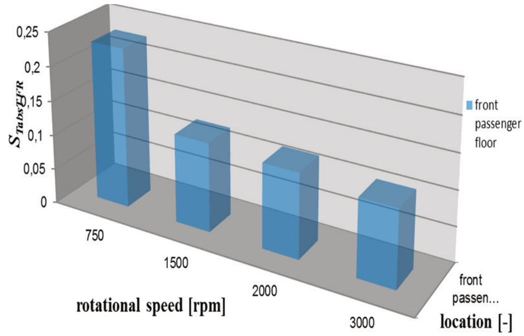

d) Front passenger floor $S_{TabsTFR}$

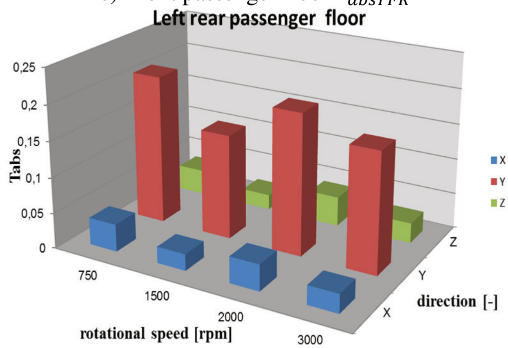

e) Left rear passenger floor T_{absTFR}

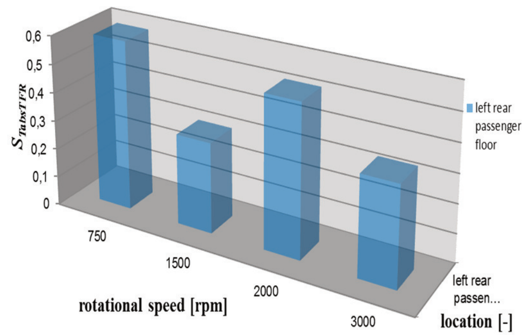

f) Left rear passenger floor $S_{TabsTFR}$

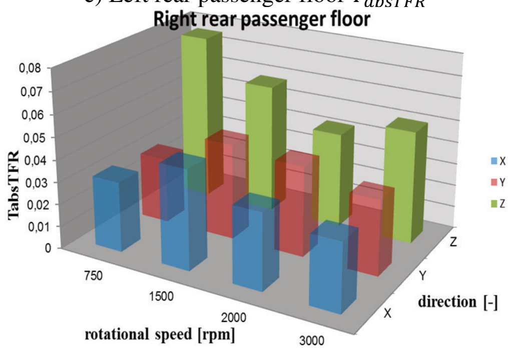

g) Right rear passenger floor T_{absTFR}

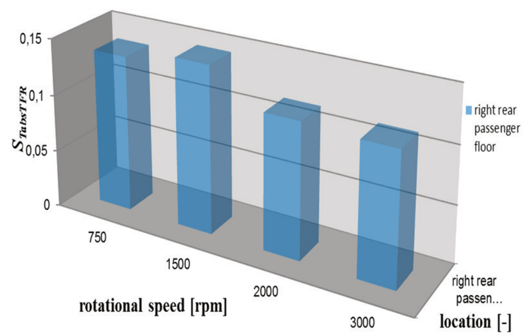

h) Right rear passenger floor $S_{TabsTFR}$

Fig. 13.42. Distribution of frequency energy floor panel vibration estimators T_{absTFR} and $S_{TabsTFR}$ for different engine rotational speed